# Tungsten Disulfide-based Ultra-Thin Solar Cells for Space Applications

Sayan Roy and Peter Bermel

Abstract-2D materials such as Transition Metal Di-Chalcogenides (TMDCs) are strong candidates for space photovoltaics, as they are very lightweight, flexible and resilient to ionizing radiation. Here, an ultra-thin tungsten disulfide (WS2) based photovoltaic cell with photon management features has been modeled, with performance improvement from enhanced absorption. Our photovoltaic model consists of a 200 nm thick WS2-based heterojunction solar cell, similar to the HIT (heterojunction with intrinsic thin layer) solar cell structure, together with a light trapping grating structure and an antireflection coating layer. The photovoltaic cell with an optimized 1-D grating light trapping structure and an appropriate antireflection dielectric coating was demonstrated to give an efficiency above 23% under the AM0 solar spectrum in our model comparable to other single-junction space photovoltaic cells. The material properties are taken directly from experimentally observed results; the proposed device architecture with additional optical features is based on experimentally fabricated devices and structures, and is expected to be resistant to ionizing radiation in the space environment. Our results show that our TMDC-based photovoltaic system with light trapping and anti-reflection coating is a strong candidate for space photovoltaic applications.

Index Terms—transition metal di-chalcogenides (TMDCs), space photovoltaics, light trapping, anti-reflection coating, absorption enhancement, radiation resistance.

#### I. INTRODUCTION

HOTOVOLTAICS is a growing and important alternative to conventional energy sources on Earth and outer space. In fact, it is the primary electric power source in outer space for Earth-orbiting satellites and many space exploratory missions, since refueling is difficult, and the solar illumination is more intense in outer space. Solar cells not only provide cheap and convenient power supply, but they also offer long-term output and reliability for extended satellite operations. In space photovoltaics, high conversion efficiency, together with light weight, is desired because of limited area and weight restrictions. An important and necessary feature is resistance to radiation-induced degradation in space environment, since the presence of large concentrations of high energy particles and cosmic rays can significantly damage solar cells. Long-term operational reliability is vital implementation in long-range space missions [1].

Until recently, silicon-based solar cells were most commonly used in space with efficiencies around 14-15% [1]. More recently, there have been steady advances in the best performing designs for the space environment. These include the incorporation of complex light trapping structures, advanced anti-reflection coatings and improved radiation tolerance. These improvements have led to high efficiency solar cells based on GaAs with efficiencies around 18-19% [2]. Now,

there is a high demand for the development of space photovoltaic systems with efficiencies above 20% [1], [3]. Space photovoltaic modules consisting of III-V multi-junction solar cells have been studied and demonstrated to exhibit efficiencies above 30% [4], [5]. Such high efficiencies are beyond the scope of single-junction technology. The goal of this project is to present a single-junction ultra-thin solar cell with performance comparable to existing single-junction solar cells. The key focus is on ultra-thin device structure using a new material, with lower mass, reduced cost, flexible features, and enhanced radiation tolerance, together with competitive performance among similar devices.

In addition to high efficiencies, recent research has focused on developing space solar cells with ultra-thin active materials and high radiation resistance. Two-dimensional (2D) transition metal di-chalcogenides (TMDCs) are the perfect candidate for future implementation in space photovoltaic technology due to their unique potential features and benefits. TMDCs are flexible, robust and can be fabricated with atomic-scale thickness. They have promising electronic and optical properties suitable for applications in photovoltaics [6], [7].

2D TMDCs can achieve significantly higher sunlight absorption per unit volume than commonly used solar absorbers such as GaAs and Si [8], allowing for lightweight and flexible PV modules. Tungsten disulfide (WS<sub>2</sub>), a 2D layered TMDC, has strong potential for solar cell applications. It has excellent absorption and carrier transport properties. It is vitally important to develop solar cell materials that have a high degree of resistance and resilience to high energy particles and cosmic rays, to maximize the end-of-life performance of the solar cell [9]. TMDCs have a high degree of resistance to radiationinduced damage; nanoelectronic devices based on TMDCs exhibit negligible degradation in performance on exposure to high energy radiation in space environment. Therefore, they have strong potential for implementation in space-based electronic and optical devices, and are particularly good candidates for space photovoltaic applications [10].

In ultra-thin solar cells, the major factor limiting efficiencies is the reduced absorption of incident photons in the solar spectrum. There has been extensive research on absorption enhancement through light trapping by sophisticated optical arrangements and complex structures [11], [12]. Light trapping can enhance the optical absorption in a solar cell and, at the same time, decrease the active layer thicknesses, which results in lightweight, low-dimensionality and high efficiency devices [13]. Thinner devices allow for improved collection of generated carriers, with less constraints on the minority carrier diffusion lengths.

This work was supported in part by the National Science Foundation (grants EEC1454315-CAREER, EEC-1227110, and CBET-1855882) and the Office of Naval Research (grant N00014-19-S-B001). *Corresponding author: Sayan Roy* 

The authors are affiliated to the School of Electrical and Computer Engineering (Birck Nanotechnology Center), Purdue University, West Lafayette, IN 47907, USA (Email: roy1@purdue.edu, pbermel@purdue.edu).

Many sophisticated arrangements and complex structures have been developed to extend the effective path length of light as optical confinement or light trapping. In photovoltaics, light trapping is used to reduce the thickness of the cell without lowering its light absorption. With an appropriate light trapping structure, a thinner solar cell can retain high absorptivity and also have a higher open-circuit voltage [14]–[16].

In almost all semiconductor materials, a significant portion of broadband incident spectrum is lost to surface reflection. Silicon, for example, has a high surface reflection of over 30% [17]. This loss of incident photons can be reduced by a great extent by incorporating a suitable dielectric material layer to function as an anti-reflection coating which minimizes surface reflection for a range of wavelengths in the incident solar spectrum [14]. In solar cells with highly absorptive materials, this substantially improves the efficiency of the device.

Here, an ultra-thin WS<sub>2</sub>-based photovoltaic model has been developed for space applications. It is beneficial to have the total active layer thickness around 100-200 nm to minimize radiation damage [17], [18]. Solar cells with active layers of thickness around microns are prone to significant damage from high energy radiation and particles in the outer space environment [19]; while ultra-thin materials with thicknesses of around few hundred nanometers are much more resistant to radiation damage with less degradation in their long-term performances [11]. Considering the possible structural damage of the material from radiation and corresponding degradation of performance, our device models were investigated with thickness limit of around 200 nm.

Next, additional features were introduced to the 200 nm-thick baseline structure to realize efficiencies above 20%. A light trapping structure and an anti-reflection coating layer were incorporated in our photovoltaic model to increase absorption of the incident solar illumination. These additional optical features lead to enhancement of the short-circuit current ( $J_{SC}$ ), and a very small increase in the open-circuit voltage ( $V_{OC}$ ). The baseline photovoltaic model with thickness of 200 nm yields efficiencies of 15.8% at 40°C and 14.3% at 70°C, which is the temperature range of satellite orbits; this is much lower than efficiencies of current space photovoltaic technology.

An optimized 1D silver grating light trapping structure was used to increase the optical path length inside the solar cell, thereby enhancing photon absorption and the  $J_{SC}$ . The efficiencies of our solar cell increased to 20.4% at 40°C and 18.5% at 70°C. In addition to light trapping, an appropriate dielectric layer was also added to function as an anti-reflection coating for reduction of surface reflection from our solar cell. This led to further increase in the  $J_{SC}$  from the additional photon absorption. The efficiencies of our final solar cell model increased to 23.6% at 40°C and 21.4% at 70°C.

Some preliminary estimates of the radiation resistivity of  $WS_2$  in comparison to common semiconductor materials have also been presented. The proton stopping power of  $WS_2$  was analyzed for high-energy protons. From the proton stopping power, the mean range, or continuous slowing down approximation (CSDA) range, was calculated at the different energies to understand the penetration depth of high energy

protons. The results were compared to those of silicon (commonly used in photovoltaics) and lead (high radiation-resistance). It was found that our ultra-thin solar cell model has much better resilience than conventional solar cells with thicknesses around few microns, for high energy protons (i.e., ionized hydrogen atoms) in the space environment.

#### II. THEORY AND METHODS

#### A. Photovoltaic Model

A solar cell model starts with a p-n junction device design to generate electron-hole pairs from incoming photons in the incident solar illumination [20]. A 3-layer device architecture was investigated for our photovoltaic model where the top layer is a thin highly-doped layer (n-type), the middle layer is a relatively thick intrinsic or light-doped layer (p-type), and the bottom layer is a thin highly-doped layer (p-type), similar to a silicon HIT solar cell structure. The electronic and optical properties of monolayer and bulk WS2 used in the device simulations include the electronic band structure, bandgap, absorption coefficient, conduction band effective density of states  $N_C$ , valence band effective density of states  $N_V$ , carrier lifetimes and relative dielectric constant. The electronic band structure and absorption profile of WS<sub>2</sub> were obtained using Density Functional Theory calculations and validated against experimentally established results. These parameters were taken from our previous work, as summarized in Table 1 [21].

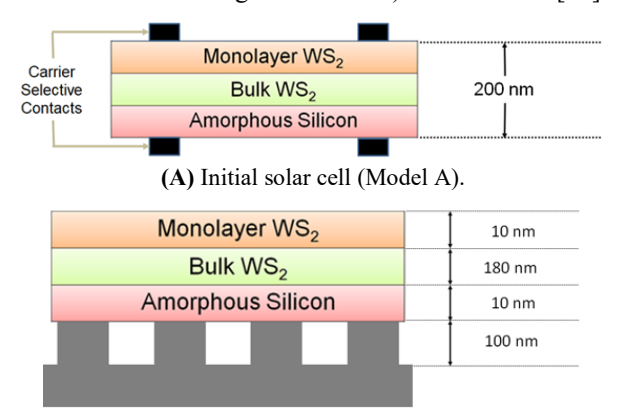
TABLE 1
Properties of monolayer WS<sub>2</sub>, bulk WS<sub>2</sub> and a-Si at 300K.

	Monolayer WS <sub>2</sub>	Bulk WS <sub>2</sub>	a-Si
Bandgap (eV)	2.15	1.29 (indirect)	1.7
Electron Affinity (eV)	(direct) 4.7	4.5	(direct) 4
Relative Dielectric Constant	5.1	13.4	11.7
N <sub>C</sub> (cm <sup>-3</sup> )	$0.97x10^{19}$	$2.02x10^{19}$	$2.82 \times 10^{19}$
Nv (cm <sup>-3</sup> )	$1.34 \times 10^{19}$	$2.48x10^{19}$	$2.65 \times 10^{19}$
Electron Mobility(cm <sup>2</sup> V <sup>-1</sup> s <sup>-1</sup> )	200	200	1
Hole Mobility(cm <sup>2</sup> V <sup>-1</sup> s <sup>-1</sup> )	50	50	0.003

The best-performing photovoltaic model in terrestrial conditions obtained in our previous work is defined as Model A, as shown in Fig. 1(A). It consists of three-layers in an  $n^+$ -pp<sup>+</sup> junction stack. The top layer is a thin layer of highly-doped n-type monolayer WS<sub>2</sub> stack; the middle layer is a thick layer of lightly-doped (almost intrinsic) p-type bulk WS<sub>2</sub>; and the bottom layer is a thin layer of highly-doped p-type amorphous silicon (a-Si). The total thickness of our device is limited to 200 nm. The optimal device structure is summarized in Table 2.

Our device simulations utilize the AM0 space solar spectrum to predict the performance and features of our WS<sub>2</sub>-based solar cell model in potential space photovoltaic applications [22]. Since the average temperature range of most satellite orbits is between 40-70°C [1], temperature values within this range were used for the device model simulations. The output current from the solar cell and the voltage across the terminals were calculated using the Drift-Diffusion model in the tool ADEPT

(A Device Emulation Program and Tool) on nanoHUB [23].



1-D Grating Structure with Silver
Grating Period = 210 nm

(B) Solar cell with light trapping grating structure and vacuum voids (Model B).



1-D Silver Grating

(C) Solar cell with light trapping and anti-reflection coating layer (Model C).

Fig. 1. Photovoltaic device models

TABLE 2 Summary of device structure for Model A.

	Top Layer	Middle Layer	<b>Bottom Layer</b>
Material	Monolayer WS <sub>2</sub>	Bulk WS <sub>2</sub>	a-Si
Bandgap (eV)	2.15	1.29	1.7
Doping Type	N	P	P
Doping conc. (cm <sup>-3</sup> )	$0.95 x 10^{19}$	$5x10^{17}$	$2.65 \times 10^{19}$
Thickness (nm)	10	180	10

Additional modifications and features were incorporated in our initial photovoltaic model to enhance absorption of the incident solar illumination, and correspondingly increase the device performance efficiency. Light trapping and anti-reflection coating were added to our initial device to obtain improved device performance. The final device structure of our photovoltaic system is shown in Fig. 1(C).

The initial solar cell together with light trapping and antireflection coating was simulated using S4sim (Stanford Stratified Structure Solver), freely available on nanoHUB [24]– [26], to obtain the absorptivity of our device. S4sim was used to analyze the improved optical performance and absorption profiles after incorporation of additional optical features. S4sim on nanoHUB has been demonstrated to be capable of reproducing published experimental research results [24].

S4 is a frequency domain code to solve the linear Maxwell's equations in layered periodic structures. Internally, it uses Rigorous Coupled Wave Analysis (RCWA, also called the

Fourier Modal Method (FMM)) and the S-matrix algorithm [16]. This tool allows for fast and accurate prediction of optical propagation (transmission, reflection and absorption spectra) in structures composed of periodic, patterned, or planar layers.

### B. Light Trapping Structure

An optimum solar cell structure with light trapping is one in which the optical path length is at least several times the actual device thickness, where the optical path length of a device is the distance that an unabsorbed photon travels within the device before it escapes out of the device [27]. Optically thin absorbers support discrete guided modes, with a photonic mode density that is dependent on the thickness and material properties of the film. The maximum enhancement is reduced as the number of available guided modes is decreased [28]. Periodic grating structures can couple diffracted light into specific modes within a narrow wavelength range.

One-dimensional (1D) surface gratings have become one of the most studied diffractive structures used in light trapping [29]. Simple grating lines diffract the incident light to the absorbing material and significantly increase the interaction length of long wavelength photons. An appropriately designed 1D grating structure can significantly enhance the absorption of the incident photons around the band edge [30].

In this work, a 1D grating structure composed of silver was considered for light trapping in our solar cell Model B; silver is highly reflective, and is widely used in a variety of photovoltaic systems. A wide range of light trapping geometric parameters were investigated, particularly focusing on grating periods and heights. The optimal light trapping structure was obtained by investigating the grating period and height which gave the maximum absorption enhancement of the AM0 solar spectrum. For each light trapping geometry, the device performance of our solar cell was obtained and compared to the cases with and without the silver grating. The maximum absorption enhancement was obtained from the grating with a height of 100 nm; the optimal grating period was found to be 210 nm.

The simulations of our device model with the light trapping structure were performed using S4sim to obtain absorption enhancement of the incident solar illumination [24]. The dielectric function of silver was obtained from the PhotonicsDB tool on nanoHUB [31]–[33]. Convergence tests were carried out for the RCWA simulations with S4. We tested our simulations for a range of Fourier orders; consistent converged results were obtained when using 99 Fourier orders.

#### C. Anti-Reflection Coating Layer

Anti-reflection coatings consist of a thin layer of dielectric material, with a specially chosen refractive index and thickness, such that interference effects in the coating cause the wave reflected from the top surface of the dielectric to be out-of-phase with the wave reflected from the semiconductor surface, thus minimizing the reflected energy [14]. Front coatings generalize this concept by including reflections from the back surface, which is particularly important for thin absorber layers.

A suitable dielectric layer with the appropriate refractive index and thickness was used in Model C. This enabled us to

study absorption enhancement realized by introducing the front coating. The refractive index of WS<sub>2</sub> is around 3 for incident photons of energies 1.5-3 eV which corresponds to the region of high intensity in the AM0 solar spectrum [34]. A dielectric layer with a refractive index of 1.5 was chosen, which is similar to glass (SiO<sub>2</sub>). Our proposed anti-reflection coating material is Spin-on-Glass (SOG) which can be accurately and uniformly deposited as a coating layer with sub-micron thickness on various semiconductor materials [35].

The thickness of the front coating was chosen to minimize net surface reflection for maximum enhancement of the incident spectrum absorption. The starting thickness of the dielectric layer was taken as 100 nm and the additional absorption enhancement in the device was investigated. The optimal dielectric layer was obtained by investigating the material thickness which gave the maximum enhancement of absorption of the AM0 solar spectrum. Various thicknesses ranging from 100 nm to 200 nm were investigated; it was found that a thickness of 150 nm for the dielectric layer gives the best absorption enhancement by minimizing surface reflection.

The simulations of the device model with the anti-reflection coating layer were carried out using S4sim [24]. The dielectric function of the anti-reflection coating material was obtained from the PhotonicsDB tool on nanoHUB [31].

#### D. Device Performance Enhancement

Initially, only our primitive solar cell Model A with the active layers, as shown in Fig. 1(A), was simulated to obtain the absorption profile and performance parameters. The dielectric functions of monolayer WS<sub>2</sub>, bulk WS<sub>2</sub> and a-Si were obtained from our prior work [21]. A suitable light trapping structure, composed of a periodic 1D silver grating with period 210 nm and height 100 nm, was then added to the solar cell. This device is denoted as Model B, as shown in Fig. 1(B). Model B was simulated to obtain the new improved absorption profile. This new absorption profile was used in the device performance simulation in ADEPT to obtain the new enhanced device efficiency and performance parameters of Model B. Our final device consists of an appropriate anti-reflection coating with a 150 nm thick dielectric layer with refractive index of 1.5, in addition to the light trapping structure. This device is denoted as Model C, as shown in Fig. 1(C). This was again simulated to obtain a further improved absorption profile. This absorption profile was used in our device simulation in ADEPT to obtain the maximally enhanced design parameters and device performance for Model C. The device models were simulated in ADEPT for the temperature range 40-70°C.

# E. Radiation Resistance Estimation

Stopping Power (S(E)) is defined as the average energy dissipated by ionizing radiation in a medium per unit path length of travel of the radiation in the medium [36]. The stopping power was obtained for high energy protons with energies 1-100 MeV, which are present in high concentrations in the outer space environment [37]. These particles have potential for maximum damage to the electronic materials and device performance.

$$S(E) = -\frac{dE}{dx}$$

Using the proton stopping power, the CSDA range ( $\Delta x$ ) was calculated for the protons with energies 1-100 MeV inside WS<sub>2</sub> [37]. The CSDA range closely approximates the average path length traveled by a charged particle as it slows down to rest, calculated in the continuous-slowing-down approximation. The CSDA range is obtained by integrating the reciprocal of the total stopping power with respect to energy.

$$\Delta x = \int_0^{E_0} \frac{1}{S(E)} dE$$

The values of S(E) and  $\Delta x$  for WS<sub>2</sub> were compared with those of silicon to gain an insight into radiation resistivity, and understand the potential advantages of our WS<sub>2</sub>-based ultra-thin solar cell over silicon solar cells in outer space applications. Our material was also compared with lead, which is known to be very resistant to radiation.

#### III. RESULTS AND DISCUSSION

#### A. Initial Photovoltaic Model Performance

The device performance parameters and features of Model A, namely,  $J_{SC}$ ,  $V_{OC}$  and efficiency, for temperatures 40°C and 70°C are summarized in Table 3. The efficiency is around 15.8% at 40°C and 14.3% at 70°C. The expected drop in the efficiency with temperature arises from the reduction of the  $V_{OC}$  due to an increase in the temperature [38]. These efficiency values are much lower than the efficiency of current space photovoltaic systems [39]. It is necessary for our model to have efficiencies above 20% to compete with existing single-junction technology.

TABLE 3
Performance parameters of Model A.

Temperature	40°C	70°C
Voc (V)	0.86	0.81
J <sub>SC</sub> (mA/cm <sup>2</sup> )	31.8	31.8
Efficiency (%)	15.8	14.3

The  $V_{\rm OC}$  for Model A at 40°C was 0.86 V and the  $J_{\rm SC}$  was 31.8 mA/cm², with 15.8% efficiency. The  $V_{\rm OC}$  obtained is similar to that of many conventional solar cells; the  $J_{\rm SC}$  is reasonable for a solar cell, although well below the performance of most commercial photovoltaic systems [40]. While the overall efficiency is not very high, it is a promising starting point to systematically improve our device.

#### B. Absorption Enhancement due to Light Trapping (Model B)

The maximum enhancement of the device performance was obtained for the 1D silver grating with height 100 nm and period 210 nm. The enhancement of  $J_{SC}$  for various geometries of the grating structure is summarized in Fig. 2. The absorption enhancement in Model B is shown in Fig. 4. There is significant improvement in the absorption of the incident solar illumination due to the 1D silver grating structure, which enhances light absorption in our device. When normalized with the AM0 solar spectrum irradiance [22], the improved absorption corresponds to an enhancement of the  $J_{SC}$  by about 26.4%.

The 1D silver grating diffracts the incident light back into the absorbing material which significantly increases the interaction length of long wavelength photons. The single-pass absorption of incident photons in the band edge region (1.3-1.7 eV) of the active materials in our solar cell is very low. An appropriately designed 1D silver grating structure significantly enhances light trapping of the incident photons around this energy range.

The peaks in the original absorption profile of Model A correspond to the resonance modes in the active materials which are absorbed in our device. The absorption spectrum of Model B consists of additional peaks, each corresponding to a new guided resonance. The low energy incident photons are diffracted by the 1D grating into these modes, leading to a much longer average optical path of these photons in the solar cell material, compared to the thickness of the device. The incident plane-waves diffracted by the light trapping structure are coupled into these guided modes with the 1D silver grating. The absorption of incident solar photons is strongly enhanced in the vicinity of each resonance.

However, a major limitation of a 1D grating light trapping structure is that each individual resonance has a narrow spectral width. To enhance absorption over a substantial portion of the solar spectrum and obtain broadband absorption enhancement, it is essential to design a more complex light trapping architecture (for example, 2D gratings with grooves) to create significantly wider and more numerous peaks over the energy range of the incident solar illumination. Although we could have investigated much finer and complex grating geometries, we decided to limit our features to measurements of 100 nm or higher to account for experimental considerations. We took these measures to propose models which are consistent with experimentally fabricable and measurable devices.

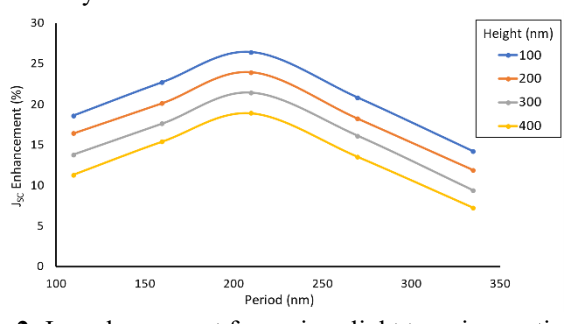


**Fig. 2.** J<sub>SC</sub> enhancement for various light trapping grating heights and periods.

# C. Absorption Enhancement due to Anti-Reflection Coating (Model C)

The  $J_{SC}$  enhancement for various thicknesses of the dielectric layer ranging from 100 nm to 200 nm is summarized in Fig. 3. The maximum enhancement of the device performance was obtained for a 150 nm thick anti-reflection coating layer. The absorption enhancement in Model C is shown in Fig. 4. There is significant improvement in the absorption of the incident solar spectrum due to the additional dielectric layer which reduces surface reflection. When normalized with the AM0 solar spectrum irradiance, the improved absorption corresponds to an enhancement of the  $J_{SC}$  by 15.4%.

Since our photovoltaic model structure consists of ultra-thin materials, the system is very responsive to the effect of the additional anti-reflection coating layer. There are several local maxima in the original absorption profile, which correspond to the resonance modes of the materials. There are also several local minima, which correspond to high surface reflection from the material. Due to the effect of the dielectric layer, there is a change in the absorption peaks of the material; the resonance modes are shifted which accounts for higher absorption of the previously lower absorption minima in the absorption profile. The surface reflection for photons in the local minima wavelengths is greatly reduced, which leads to the formation of new absorption peaks in the enhanced absorption profile, resulting from changes in the resonance modes.

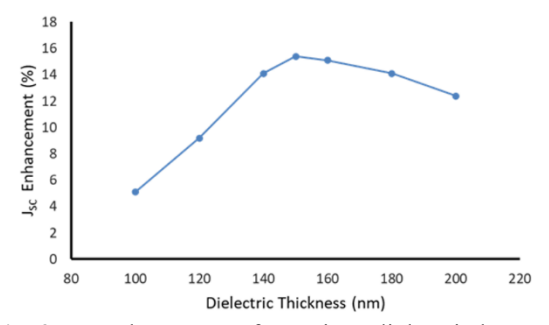


**Fig. 3.** J<sub>SC</sub> enhancement for various dielectric layer thicknesses.

In our anti-reflection coating, there is room for possible further reduction of surface reflection. It may be possible, in future work, to design and fabricate a perfect anti-reflection coating layer using complex dielectric architecture to obtain even lower reflection of the incident spectrum.

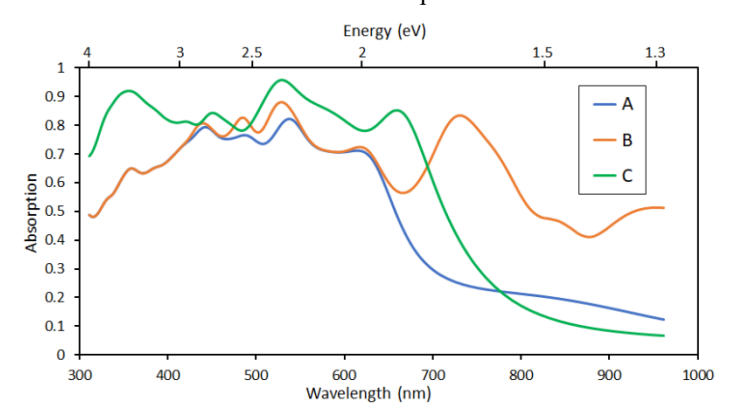


**Fig. 4.** Absorption enhancement with light trapping (Model B) and anti-reflection coating (Model C), and initial absorption (Model A).

# D. Performance Enhancement of Photovoltaic System

The performance parameters of our photovoltaic models (A, B and C), such as  $J_{SC}$ ,  $V_{OC}$  and efficiency, were recorded for temperatures 40°C (Table 4), 50°C (Table 5), 60°C (Table 6) and 70°C (Table 7). The current-voltage relationship of our models, showing the  $J_{SC}$  and  $V_{OC}$ , are shown in Fig. 5 (40°C) and Fig. 6 (70°C).

For Model B, the  $V_{OC}$  was 0.87 V and the  $J_{SC}$  was 40.2 mA/cm², with 20.4% efficiency. This enhancement of the  $J_{SC}$ , and correspondingly efficiency, is the result of improved absorption of the incident solar illumination from the light trapping structure. Compared to Model A, the  $J_{SC}$  increases

greatly by about 26%; the efficiency of the device Model B is significantly higher than A, and is comparable to commercial solar cells. The results are very promising, but it is possible to improve the device even further, since there are still losses due to surface reflection of the incident photons.

TABLE 4
Performance parameters of device models A, B and C at 40°C.

Model	A	В	С
Voc (V)	0.86	0.87	0.87
$J_{SC}$ (mA/cm <sup>2</sup> )	31.8	40.2	46.4
Fill Factor	0.79	0.80	0.81
Efficiency (%)	15.8	20.4	23.6

TABLE 5
Performance parameters of device models A, B and C at 50°C.

Model	A	В	С
Open Circuit Voltage V <sub>OC</sub> (V)	0.85	0.85	0.85
J <sub>SC</sub> (mA/cm <sup>2</sup> )	31.8	40.2	46.4
Fill Factor	0.78	0.79	0.80
Efficiency (%)	15.3	19.7	22.8

TABLE 6
Performance parameters of device models A, B and C at 60°C.

Model	A	В	С
Voc (V)	0.83	0.83	0.83
J <sub>SC</sub> (mA/cm <sup>2</sup> )	31.8	40.2	46.4
Fill Factor	0.77	0.78	0.79
Efficiency (%)	14.8	19.1	22.1

TABLE 7
Performance parameters of device models A, B and C at 70°C.

Model	A	В	C
Open Circuit Voltage V <sub>OC</sub> (V)	0.81	0.82	0.82
J <sub>SC</sub> (mA/cm <sup>2</sup> )	31.8	40.2	46.4
Fill Factor	0.76	0.77	0.78
Efficiency (%)	14.3	18.5	21.4

The performance of Model C is found to be much improved because of additional absorption arising from reduction of surface reflection. The  $V_{\rm OC}$  was 0.87 V and the  $J_{\rm SC}$  was 46.4 mA/cm², with 23.6% efficiency. The  $J_{\rm SC}$  is much better than the previous structures (A and B), and has increased significantly (by about 46% relative, compared to Model A). The performance trends are similar for temperature of 70°C. Model A has  $V_{\rm OC}$  0.81 V,  $J_{\rm SC}$  31.8 mA/cm², with 14.3% efficiency. Model B has  $V_{\rm OC}$  0.82 V,  $J_{\rm SC}$  40.2 mA/cm², with 18.5% efficiency. Model C has  $V_{\rm OC}$  0.87 V,  $J_{\rm SC}$  46.4 mA/cm², with 21.4% efficiency. This enhancement of the  $J_{\rm SC}$ , and correspondingly efficiency, is the result of improved absorption of the incident solar illumination from the light trapping structure and anti-reflection coating layer.

The efficiency of Model C is comparable to some of the previously developed high-efficiency single junction solar cells

under AM0 spectrum, namely, solar cells based on silicon (20.8%), GaAs (21.8%) and InP (19.9%) [3]. For a better comparison to the current best-performing single-junction solar cells, we have also simulated our solar cell model under the AM1.5 terrestrial solar spectrum at 25°C. The efficiency of our device (Model C) was found to be 26.9%. This is similar to the highest performance crystalline silicon solar cell which has an efficiency of 26.7% [40]. In addition, our solar cell efficiency is slightly below the best performing single-junction terrestrial solar cell, which is based on GaAs with an efficiency of 29.1% [40].

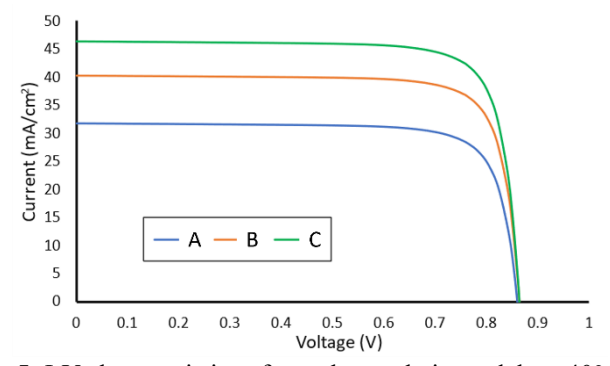
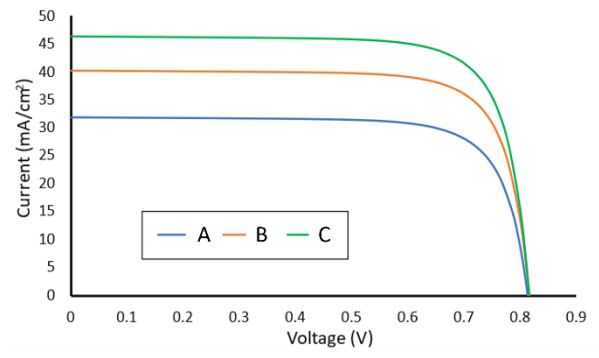


Fig. 5. J-V characteristics of our photovoltaic models at 40°C.



**Fig. 6.** J-V characteristics of our photovoltaic models at 70°C.

The goal of increasing the device performance efficiency is through enhancement of the  $J_{SC}$ ; mechanisms of significantly increasing the  $V_{OC}$  were not explored here. In addition, there is no significant deterioration of the intrinsic bandgap of WS<sub>2</sub> due to increase in the temperature. For a temperature increase from  $40^{\circ}\text{C}$  to  $70^{\circ}\text{C}$ , the bandgap of WS<sub>2</sub> reduces by around 8-9 meV, which is similar to the drop in bandgap energy for silicon [38].

These results create new possibilities for fabrication and use of ultra-thin high-efficiency solar cells for space photovoltaic applications using a new 2D material which has the advantages of ultra-low weight per unit of power production, mechanical flexibility, resilience and reliability, compared to several commonly-used photovoltaic materials.

## E. Radiation Resistance of WS2

The stopping power for high energy protons with energies 1-100 MeV were obtained from existing sources, as shown in Fig. 7 [37]. The CSDA range ( $\Delta x$ ) of the protons are summarized in Fig. 8. For protons with energies of 10-100 MeV, the stopping power of WS<sub>2</sub> is almost double that of silicon. For comparison, the stopping power of lead is about three times of silicon. The

CSDA ranges of protons with energies 10-100 MeV in silicon is almost twice that of  $WS_2$  and about thrice that of lead.

If we compare a 10  $\mu$ m thick silicon solar cell and our 200 nm WS<sub>2</sub>-based device, the silicon cell is about 50 times thicker than our model. The energy decay of protons in a material can be approximated as a linear dissipation of energy as the proton passes through the device, based on the stopping power of the material. For a 10 MeV proton, the stopping power of silicon is 80.6 MeV/cm and that of WS<sub>2</sub> is 136.5 MeV/cm. The total energy dissipated in a 10  $\mu$ m thick silicon structure is about 80.6 eV, while the total energy dissipated in our 200 nm thick WS<sub>2</sub> device is about 2.7 eV. The energy dissipated in WS<sub>2</sub> is roughly 30 times less than that of silicon for 10 MeV protons. The estimated reduction in energy dissipation in our solar cell is around a factor of 40 for 1 MeV protons and a factor of 25 for 100 MeV protons, using a similar analysis.

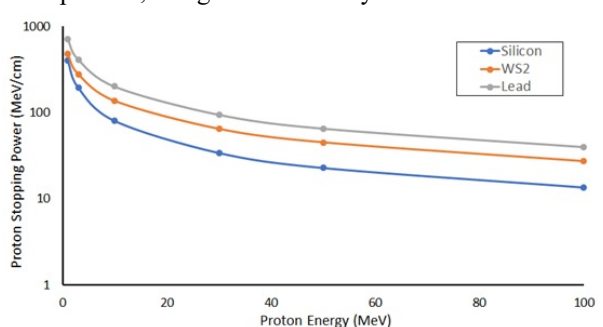


Fig. 7. Proton stopping powers for silicon,  $WS_2$  and lead (MeV/cm).

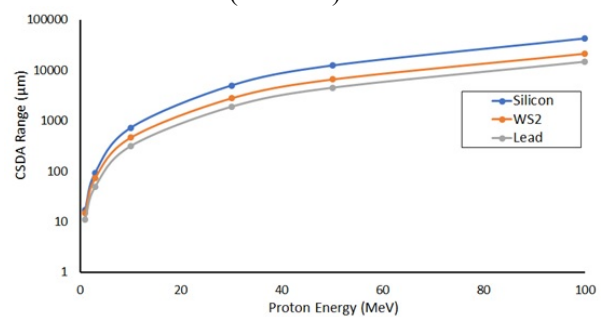


Fig. 8. CSDA ranges for silicon, WS<sub>2</sub> and lead ( $\mu$ m).

From these preliminary calculations, it can be estimated that our 200 nm  $WS_2$  device is around 25-40 times more resistant to high energy radiation (1-100 MeV protons) than the 10  $\mu$ m silicon device due to the ultra-thin structure. The most significant benefit of choosing an ultra-thin device is the reduction of radiation damage due to lesser energy dissipation of high energy particles in the material. Our 200 nm thick device will absorb only a fraction of high energy radiation compared to devices with thicknesses of the order of microns. Thus, by using an ultra-thin  $WS_2$ -based solar cell, we can achieve significant enhancement of the radiation resistivity in the space environment.

It has been demonstrated in recent studies that solar cells with thicknesses of the order of a micron are prone to significant damage from high energy radiation [18]. The primary reason for degradation is the reduction of minority carrier diffusion lengths on exposure to radiation. This leads to loss of free carriers due to recombination in the material, and

correspondingly reduced carrier collection efficiency at the end contacts. However, a solar cell with thickness of around 100-200 nm is much more resistant to this effect. Even with reduction of the minority carrier diffusion length, these devices are enough thin for efficient carrier collection. Since our device has a thickness of 200 nm, we expect there won't be significant degradation of performance due to reduction of the minority carrier diffusion lengths, as most of the generated carriers will be collected efficiently at the end contacts.

#### IV. CONCLUSION

In this work, a solar cell model based on tungsten disulfide (WS<sub>2</sub>) has been developed for proposed implementation in space photovoltaics. Our model consists of a 200 nm thick WS<sub>2</sub>based solar cell, together with a light trapping structure consisting of a 1D silver grating, and an appropriate dielectric material layer to function as an anti-reflection coating. The device performance of our final photovoltaic model was 23.6% at 40°C and 21.4% at 70°C. The estimate of radiation absorption and energy dissipation shows that our ultra-thin solar cell is much more resilient to high energy radiation, as compared to solar cells with thicknesses of the order of microns. Since our model has been tied directly into experimental observations, this WS<sub>2</sub> based photovoltaic device can be competitive and comparable to the performance of existing single-junction solutions, while adding natural advantages in terms of light weight, flexibility, earth abundance and resilience.

#### REFERENCES

- [1] P. A. Iles, "Future of photovoltaics for space applications," Progress in Photovoltaics: Research and Applications, vol. 8, no. 1, 2000, doi: 10.1002/(SICI)1099-159X(200001/02)8:1<39::AID-PIP304>3.0.CO;2-D.
- [2] A. Vijh, L. Washington, and R. C. Parenti, "High Performance, Lightweight GaAs Solar Cells for Aerospace and Mobile Applications," 2018. doi: 10.1109/pvsc.2017.8366342.
- 3] S. G. Bailey and D. J. Flood, "Space photovoltaics," *Progress in Photovoltaics: Research and Applications*, vol. 6, no. 1, 1998, doi: 10.1002/(sici)1099-159x(199801/02)6:1<1::aid-pip204>3.3.co;2-o.
- [4] J. Li et al., "A Brief Review of High Efficiency III-V Solar Cells for Space Application," Frontiers in Physics, vol. 8. 2021. doi: 10.3389/fphy.2020.631925.
- [5] R. R. King et al., "Advanced III-V multijunction cells for space," in Conference Record of the 2006 IEEE 4th World Conference on Photovoltaic Energy Conversion, WCPEC-4, 2006, vol. 2. doi: 10.1109/WCPEC.2006.279831.
- [6] Q. H. Wang, K. Kalantar-Zadeh, A. Kis, J. N. Coleman, and M. S. Strano, "Electronics and optoelectronics of two-dimensional transition metal dichalcogenides," *Nature Nanotechnology*, vol. 7, no. 11. 2012. doi: 10.1038/nnano.2012.193.
- [7] S. M. Auerbach, K. A. Carrado, and P. K. Dutta, *Handbook of Layered Materials*. 2004. doi: 10.1201/9780203021354.
- [8] M. Bernardi, M. Palummo, and J. C. Grossman, "Extraordinary sunlight absorption and one nanometer thick photovoltaics using two-dimensional monolayer materials," *Nano Letters*, vol. 13, no. 8, 2013, doi: 10.1021/nl401544y.
- [9] R. J. Walters, S. Messenger, J. H. Warner, C. D. Cress, M. Gonzalez, and S. Maximenko, "Modeling of radiation induced defects in space solar cells," in *Physics and Simulation of*

#### MANUSCRIPT ID: JPV-2021-12-0511

- Optoelectronic Devices XIX, 2011, vol. 7933. doi: 10.1117/12.873902.
- [10] T. Vogl et al., "Radiation tolerance of two-dimensional material-based devices for space applications," *Nature Communications*, vol. 10, no. 1, 2019, doi: 10.1038/s41467-019-09219-5.
- [11] N. Z. Vagidov, K. H. Montgomery, G. K. Bradshaw, and D. A. Wilt, "Light trapping structures for radiation hardness enhancement of space solar cells," *Solar Energy Materials and Solar Cells*, vol. 182, 2018, doi: 10.1016/j.solmat.2018.03.036.
- [12] E. R. Martins, J. Li, Y. Liu, J. Zhou, and T. F. Krauss, "Engineering gratings for light trapping in photovoltaics: The supercell concept," *Physical Review B - Condensed Matter and Materials Physics*, vol. 86, no. 4, 2012, doi: 10.1103/PhysRevB.86.041404.
- [13] C. van Lare, F. Lenzmann, M. A. Verschuuren, and A. Polman, "Dielectric Scattering Patterns for Efficient Light Trapping in Thin-Film Solar Cells," *Nano Letters*, vol. 15, no. 8, 2015, doi: 10.1021/nl5045583.
- [14] T. Markvart and L. Castañer, "Principles of solar cell operation," in McEvoy's Handbook of Photovoltaics: Fundamentals and Applications, 2018. doi: 10.1016/B978-0-12-809921-6.00001-X.
- [15] M. van Eerden *et al.*, "A facile light-trapping approach for ultrathin GaAs solar cells using wet chemical etching," *Progress in Photovoltaics: Research and Applications*, vol. 28, no. 3, 2020, doi: 10.1002/pip.3220.
- [16] L. Li, "Formulation and comparison of two recursive matrix algorithms for modeling layered diffraction gratings," *Journal of the Optical Society of America A*, vol. 13, no. 5, 1996, doi: 10.1364/josaa.13.001024.
- [17] M. A. Green and M. J. Keevers, "Optical properties of intrinsic silicon at 300K," *Progress in Photovoltaics: Research and Applications*, vol. 3, no. 3, 1995, doi: 10.1002/pip.4670030303.
- [18] L. C. Hirst et al., "Intrinsic radiation tolerance of ultra-thin GaAs solar cells," Applied Physics Letters, vol. 109, no. 3, 2016, doi: 10.1063/1.4959784.
- [19] I. Massiot, A. Cattoni, and S. Collin, "Progress and prospects for ultrathin solar cells," *Nature Energy*, vol. 5, no. 12. 2020. doi: 10.1038/s41560-020-00714-4.
- [20] M. A. Green, "Photovoltaic principles," in *Physica E: Low-Dimensional Systems and Nanostructures*, 2002, vol. 14, no. 1–2. doi: 10.1016/S1386-9477(02)00354-5.
- [21] S. Roy and P. Bermel, "Electronic and optical properties of ultrathin 2D tungsten disulfide for photovoltaic applications," *Solar Energy Materials and Solar Cells*, vol. 174, Jan. 2018, doi: 10.1016/j.solmat.2017.09.011.
- [22] "Reference Air Mass 1.5 Spectra." https://www.nrel.gov/grid/solar-resource/spectra-am1.5.html (accessed Sep. 29, 2019).
- [23] J. Gray, X. Wang, R. V. K. Chavali, X. Sun, A. Kranti, and J. R. Wilcox, "ADEPT 2.1," 2015. https://nanohub.org/resources/10913/about#citethis (accessed Oct. 30, 2016).
- [24] J. Kang, X. Wang, P. Bermel, and C. Liu, "S4: Stanford Stratified Structure Solver," 2012, doi: https://doi.org/10.4231/D35T3G11T.
- [25] V. Liu and S. Fan, "S4: A free electromagnetic solver for layered periodic structures," *Computer Physics Communications*, vol. 183, no. 10, Oct. 2012, doi: 10.1016/j.cpc.2012.04.026.
- [26] M. Ghebrebrhan, P. Bermel, Y. Avniel, J. D. Joannopoulos, and S. G. Johnson, "Global optimization of silicon photovoltaic cell front coatings," *Optics Express*, vol. 17, no. 9, 2009, doi: 10.1364/oe.17.007505.
- [27] E. Yablonovitch and G. D. Cody, "Intensity Enhancement in Textured Optical Sheets for Solar Cells," *IEEE Transactions on Electron Devices*, vol. 29, no. 2, 1982, doi: 10.1109/T-ED.1982.20700.

- [28] F. J. Beck, A. Stavrinadis, T. Lasanta, J.-P. Szczepanick, and G. Konstantatos, "Understanding light trapping by resonant coupling to guided modes and the importance of the mode profile," *Optics Express*, vol. 24, no. 2, 2016, doi: 10.1364/oe.24.000759.
- [29] K. Li et al., "Light trapping in solar cells: simple design rules to maximize absorption," Optica, vol. 7, no. 10, 2020, doi: 10.1364/optica.394885.
- [30] Z. Yu, A. Raman, and S. Fan, "Fundamental limit of light trapping in grating structures," *Optics Express*, vol. 18, no. S3, 2010, doi: 10.1364/oe.18.00a366.
- [31] X. Ni, Z. Liu, and A. v. Kildishev, "PhotonicsDB: Optical Constants." https://nanohub.org/resources/photonicsdb (accessed Oct. 30, 2016).
- [32] E. D. Palik, *Handbook of optical constants of solids*, vol. 1. 2012. doi: 10.1016/C2009-0-20920-2.
- [33] P. B. Johnson and R. W. Christy, "Optical constants of the noble metals," *Physical Review B*, vol. 6, no. 12, 1972, doi: 10.1103/PhysRevB.6.4370.
- [34] C. Hsu et al., "Thickness-Dependent Refractive Index of 1L, 2L, and 3L MoS2, MoSe2, WS2, and WSe2," Advanced Optical Materials, vol. 7, no. 13, 2019, doi: 10.1002/adom.201900239.
- [35] F. Packeer, M. A. M. Zawawi, N. Z. I. Hashim, N. M. Noh, W. M. Jubadi, and M. Missous, "Alternative Spin-On-Glass (SoG) material characterization for Deep-Submicron (<0.35 um) soft reflow fabrication process," in *IOP Conference Series: Materials Science and Engineering*, 2018, vol. 380, no. 1. doi: 10.1088/1757-899X/380/1/012005.
- [36] M. F. L'Annunziata, "Nuclear Radiation, Its Interaction with Matter and Radioisotope Decay," in *Handbook of Radioactivity Analysis*, 2003. doi: 10.1016/B978-012436603-9/50006-5.
- [37] "PSTAR." https://physics.nist.gov/PhysRefData/Star/Text/PSTAR.html (accessed Mar. 07, 2021).
- [38] B. J. van Zeghbroeck, "Temperature dependence of the energy bandgap." https://ecee.colorado.edu/~bart/book/eband5.htm (accessed Mar. 07, 2021).
- [39] S. G. Bailey, R. Raffaelle, and K. Emery, "Space and terrestrial photovoltaics: Synergy and diversity," *Progress in Photovoltaics: Research and Applications*, vol. 10, no. 6, 2002, doi: 10.1002/pip.446.
- [40] M. A. Green, E. D. Dunlop, J. Hohl-Ebinger, M. Yoshita, N. Kopidakis, and X. Hao, "Solar cell efficiency tables (version 58)," *Progress in Photovoltaics: Research and Applications*, vol. 29, no. NREL/JA-5900-80028, 2021, doi: 10.1002/pip.3444.



Savan Roy is a post-doctoral research assistant in the School of Electrical and Computer Engineering Purdue at University. He obtained his BS degree in May 2013, MS degree in May 2017 and PhD degree in May 2021, all in Electrical and Computer Engineering from Purdue University. research

interests

include transition metal dichalcogenides (TMDCs), photovoltaics, photonics and nanoelectronics. His doctoral research topic was modeling of ultrathin 2D TMDCs for nano-electronic and photovoltaic applications and implementing advanced techniques, with a focus on tungsten disulfide, tungsten diselenide and hybrid

His



tungsten-based TMDCs.

Peter Bermel is the Elmore Associate Professor of Electrical and Computer Engineering at Purdue University. He obtained his BS degree from University of North Carolina-Chapel Hill in May 2000, MPhil degree from Cambridge University in June 2002, and PhD degree from Massachusetts Institute of Technology in May 2007.

His research focuses on improving the performance of photovoltaic, thermophotovoltaic,

and microelectronic systems using the principles of nanophotonics. Key enabling techniques for his work include electromagnetic and electronic theory, modeling, simulation, fabrication, and characterization.